EurJIC European Journal of Inorganic Chemistry

ChemPubSoc Europe

FULL PAPER

DOI:10.1002/ejic.201402220

# Supramolecular Control of Biomimetic Coordination – $Zn^{II}$ Cavity Complexes Presenting Two Differentiated Labile Sites in *cis* Positions

**Jérôme Gout,[a] Stéphanie Rat,[a] Olivia Bistri,[a] and Olivia Reinaud*[a]**

**Keywords:** Macrocycles / Biomimetic complexes / Zinc / Host–guest systems / Nitrogen heterocycles

A supramolecular approach to model the active sites of metalloenzymes is to associate a cavity with a tripodal coordination core. One key feature of many enzymes is the possible binding of two different ligands in *cis* positions relative to each other, which has not yet been described for cavity complexes. Here, the bowl shape of resorcinarene allows such a coordination environment for $Zn^{II}$ complexes. A detailed NMR study with various carboxylic acids evidences size-, shape-, and, thus, regioselectivity for carboxylate coordination in the *endo* position, the *exo* position, or both. The coordination of diketonates unambiguously demonstrates the relative *cis* position of the two labile sites present in the tris(imidazole)zinc(II) bowl complex. An interesting intramolecular exchange process was also observed. Finally, a comparison with calix[6]arene-based complexes (so-called funnel complexes) further highlights the key role of the cavity in the control of properties of the metal ion.

## Introduction

The design of artificial receptors has become a field of growing interest over recent decades. The particular case of "metallated cavitands" has recently been the subject of exhaustive reviews.[1–3] Among them, one category is of particular interest as it concerns transition metal complexes with a guest ligand embedded in a cavity. Such a design allows control of ligand binding, exchange, affinity, and reactivity by the cavity. The corresponding metal centers are under the supramolecular control of the cavity, and – in view of this specific feature – they will be here designated as "cavity complexes". Cavity complexes are based on various macrocycles such as calixarenes, cyclodextrins,[4] and glycoluril.[1] The first examples of such cavity complexes with an embedded labile ligand evidenced both in the solid state and in solution were reported in 1998 and are based on calix[6]arenes[5] and calix[4]arenes.[6] These two systems display common and different features (Figure 1). The calix[6]arene-based $Cu^{I}$ complex (and subsequently described $Zn^{II}$ complexes,[7] also called "funnel complexes")[8] displays a single exogenous[9] ligand (an organonitrile) bound to the metal center in the cavity within a tetrahedral geometry ($T_d$, Figure 1c). The $Ru^{II}$ complexes based on calix[4]arene display four exogenous ligands, one of which (CO) is embedded in the cavity (Figure 1a). Other metal complexes were described with the same scaffolds. With calix[4]arenes, square-planar complexes were obtained with $Pt^{II}$ and $Pd^{II}$ centers and two exogenous ligands in *trans* positions relative to each other, one (a hydride or a methyl group) is selectively embedded in the calixarene core.[6] $Cu^{II}$ complexes based on calix[6]arenes also form five-coordinate species with two exogenous ligands in *trans* positions (Figure 1c).[10,11] Such a *trans* pattern restricts the scope of the reactivity of the metal ion. Indeed, the presence of two labile sites in *cis* positions relative to each other is often crucial for reactivity. It allows the simultaneous binding of a substrate and a reactant or the formation of intermediates with two donor atoms bound to the metal ion. Only very few examples of cavitands with a metal center presenting two (and only two) coordination sites in *cis* positions confined at the receptor entrance have been reported.[1,12] One remarkable example concerns a (diphosphane)silver(I) complex of a cyclodextrin (CD) with two exchangeable nitrile ligands inside the cavity (Figure 1b).[13] Within the same CD framework, but associated with a tris(nitrogen) core, an $Fe^{II}$ complex displays catalytic activity for ethylene polymerization with unusual selectivity.[14] Finally, it is important to note that the two *cis* labile coordination sites are not differentiated in the above-cited examples.

A metal ion associated with a hydrophobic cavity is reminiscent of the active sites of metalloenzymes.[15] For many enzymes, the presence of two labile sites in *cis* positions rel-

[a] Laboratoire de Chimie et de Biochimie pharmacologiques et toxicologiques, Université Paris Descartes, CNRS UMR 8601
45, rue des Saints Pères, 75006 Paris, France
E-mail: Olivia.Reinaud@parisdescartes.fr
http://www.biomedicale.univ-paris5.fr/umr8601/-Chimie-Bioinorganique-.html

Supporting information for this article is available on the WWW under http://dx.doi.org/10.1002/ejic.201402220.

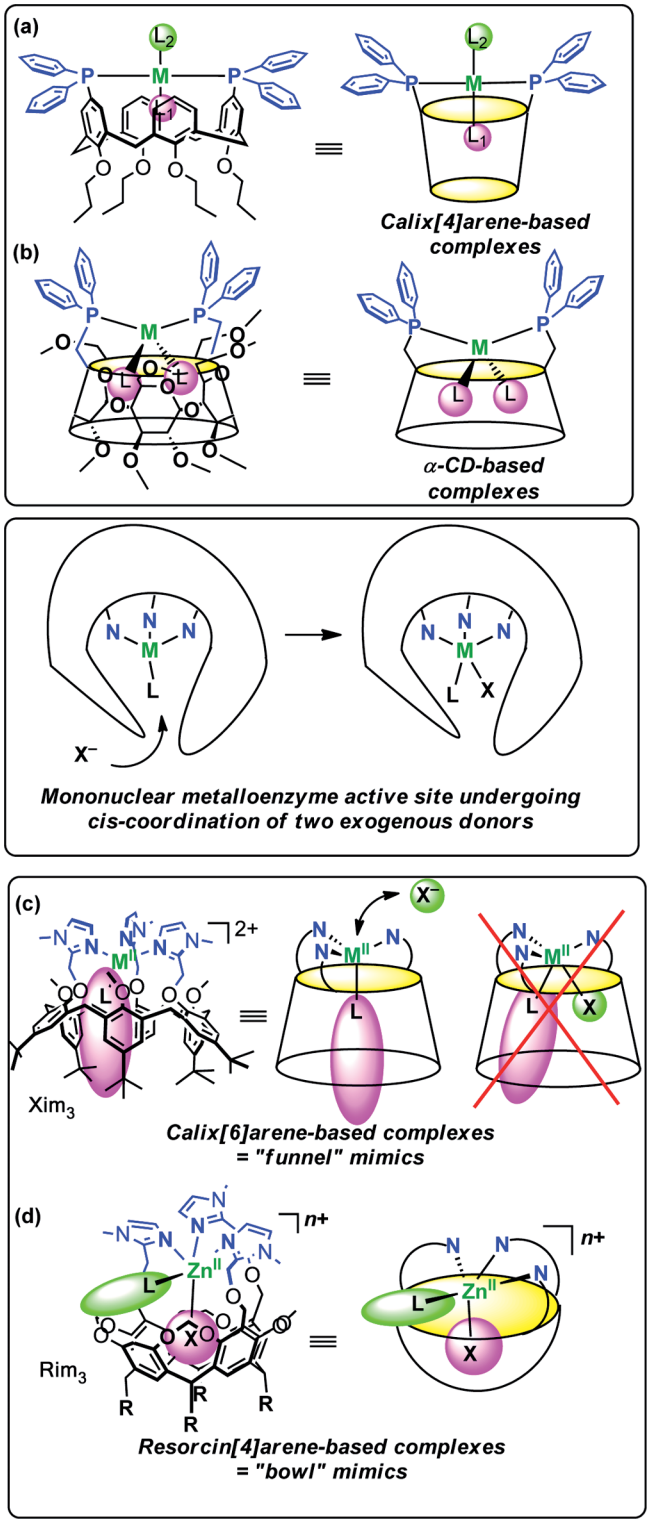


Figure 1. Top: (a, b) Cavity complexes presenting two exogenous labile sites, as reported by Matt et al. Middle: Schematized active site of mononuclear metalloenzymes. Bottom: (c, d) Cavity-based model complexes.

ative to each other is also a crucial feature for catalysis, for example, for $Zn^{II}$ hydrolases, lyases, and aldolases[16] or non-heme iron oxygenases.[17] Our group is focusing on the development of supramolecular mimics of mononuclear metalloenzymes[18] that integrate host–guest features, which are key for substrate affinity, selectivity, and reactivity. As mentioned above, we have developed model complexes based on the calix[6]arene scaffold. These cavity complexes display a nitrogen coordination core that mimics the poly(histidine) site present in many metalloenzymes and coordinates to biologically occurring metal ions such as copper and zinc.[8,19,20] In this system, the simultaneous embedment of two guest ligands is totally precluded by the small rim of the cone cavity. Hence, the only site that allows interaction with a second exogenous ligand[10,21] (or an anion)[11] is situated in a *trans* position as shown in Figure 1c.

Recently, we have reported the synthesis of a new biomimetic cavity ligand based on the resorcin[4]arene scaffold ($Rim_3$; Figure 1d).[22] The ligand presents a bowl shape with three imidazole groups attached to the large rim and stabilizes five-coordinate $Zn^{II}$ species. This coordination mode contrasts with the tetrahedral complexes obtained with calix[6]arene-based ligands ($Xim_3$; Figure 1c) functionalized at the small rim with the same tris(imidazole) tripodal core.

Preliminary studies related to the hosting properties of the $Rim_3Zn^{II}$ complex showed the selective binding of an acetate anion in the bowl cavity in the *endo* position. Here, we report an in-depth study that explores the hosting properties of this $Zn^{II}$ complex with various organic acids in the presence of a base. It highlights an impressive selectivity for *endo* binding relative to *exo* binding, which leads to the strong differentiation of the two labile sites that are in *cis* positions relative to each other.

## Results and Discussion

The $Zn^{II}$ complex based on the $Rim_3$ ligand was obtained according to the previously described procedure[22] by treating 1 equiv. of zinc perchlorate with the ligand in ethanol. In the isolated solid of formula $[Zn(Rim)(S)(ClO_4)][ClO_4]$, the $Zn^{II}$ center binds a perchlorate anion and a solvent EtOH or water molecule (S). In solution, the perchlorate anion dissociates, and a dicationic species is obtained $[Zn(Rim)(S)_2][ClO_4]_2$. We have reported the formation of a mono(acetato) complex when sodium acetate was added to a solution containing the dicationic complex, and the product has an NMR signature characteristic of *endo* binding. When $Zn(OAc)_2$ was used for the complexation to the $Rim_3$ ligand, a different complex was obtained and identified as a bis(acetato) complex. Here, we will first report a detailed study related to the coordination of acetate ions generated in solution through the simultaneous addition of acetic acid and triethylamine.

### Acetate Coordination

The interaction of the $Zn^{II}$ center with acetate ions in $CD_3CN$ was monitored by $^1H$ NMR spectroscopy. The progressive addition of tetrabutylammonium acetate led to the quantitative and sequential formation of the mono- and

 

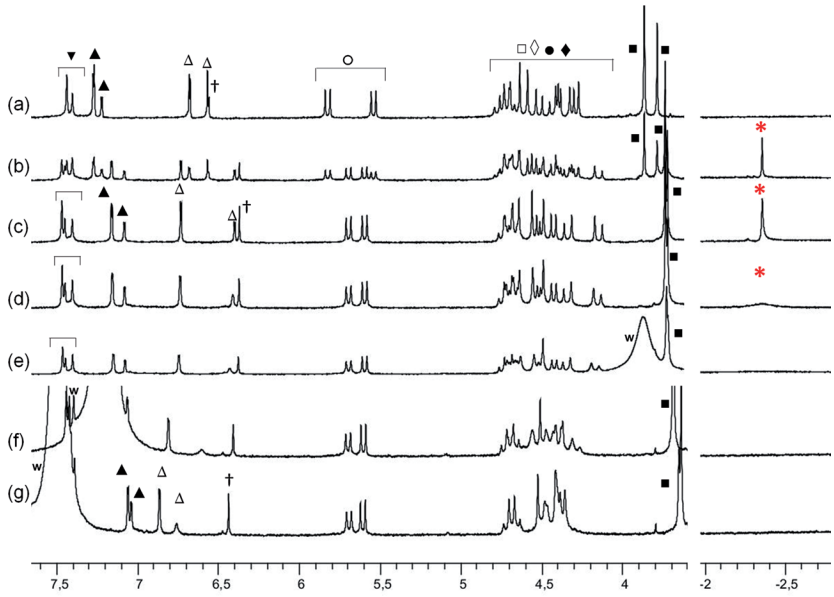


Figure 2. $^1$H NMR spectra (250 MHz, 300 K) of $[Zn(Rim)(S)_2][ClO_4]_2$ in $CD_3CN$ (3.7 mM) before (a) and after the addition of a 1:1.5 mixture of acetic acid/triethylamine: (b) 0.5, (c) 1.2, (d) 2.1, (e) 3.5 equiv. (AcOH vs. Zn), and in the presence of (f) 70 and 44 equiv. and (g) 70 and 80 equiv. of acetic acid and triethylamine, respectively. The signals annotated with a red asterisk correspond to the encapsulated guest, w stands for water. ▼ HAr "down", ▲ and Δ HIm, † HAr "up", ○ and ● $OCH_2O$, □ $CHC_5H_{11}$, ◇ $CH_2Im$, ♦ $ArCH_2O$, ■ $NCH_3$.

bis(acetato) complexes[22] after 1 and 2 equiv., respectively (Figure S1). To gain more insights into the different binding strength of the first and second acetate ion to the metal center, the experience was repeated with acetic acid in the presence of a weak base. $Et_3N$ was chosen for this purpose in view of its low p$K_a$ in MeCN relative to that of acetic acid (18.8 vs. 23.5, respectively).[23] The $^1$H NMR spectra for the titration of the $Rim_3Zn^{II}$ complex by the stepwise addition of acetic acid in the presence of triethylamine are displayed in Figure 2. Under substoichiometric conditions (Figure 2b), the appearance of a second set of signals for the $Rim_3$ ligand indicates the formation of a new single species identified as the mono(acetato) complex. An associated high-field resonance [$\delta$ = –2.43 ppm, complexation-induced shift (CIS) = –4.3 ppm] attests to the coordination of the acetate anion in the *endo* position and, hence, it responds to the π-rich environment provided by the resorcinarene cavity. This NMR signature (Figure 2b) shows a slow exchange regime (on the spectroscopic timescale) between the starting dicationic complex and the monocationic acetato adduct. Integration of the signals indicated the quantitative coordination of the acetate ion to the $Rim_3Zn^{II}$ complex. After the addition of exactly 1 equiv. of acetic acid, the starting complex was no longer detectable, and the acetato complex was the only species present in solution (Figure 2c). Such a strong complexation prevented the measurement of the affinity constant by this spectroscopy.

The addition of a second equivalent of acid did not affect the NMR profile (Figure 2d) except for the high-field-shifted peak corresponding to the embedded acetate ion. This peak considerably broadened and completely disappeared upon further addition of acid (Figure 2e–g). This can be explained by an enhancement of the guest exchange rate when the exogenous ligand is in excess, consistent with an associative exchange mechanism. This mono(acetato) complex appeared relatively reluctant to bind a second acetate ion under these experimental conditions. Indeed, the signature of the bis(acetato) complex was obtained only after the addition of a very large excess of acetic acid and $Et_3N$ (ca. 80 equiv., Figure 2g). This stands in contrast with the quantitative formation of the bis adduct upon the addition of only 2 equiv. of $n$Bu$_4$NOAc (Figure S1). Hence, these titration conditions have demonstrated a difference in the bonding strength of the first and second acetate ion to the $Zn^{II}$ center. Whereas the Lewis acidity of the metal ion of the starting dicationic complex is high enough to promote deprotonation of acetic acid by $Et_3N$ under stoichiometric conditions, the resulting decrease of Lewis acidity of the mono(acetato)zinc(II) center renders the coordination of a second acetate ion more difficult.

## Heptanoate Coordination

To evaluate the difference between *endo* and *exo* coordination, a similar titration of the $Rim_3Zn^{II}$ complex with heptanoic acid in the presence of triethylamine was conducted, and the corresponding $^1$H NMR spectra are reported in Figure 3. In this case, *endo* binding is a priori precluded as the long chain of the guest ($n$C$_6$H$_{13}$) cannot fit into the cavity. Under substoichiometric conditions, the resonances of the starting complex broadened, and new but very broad peaks became distinguishable (Figure 3b). At ca. 1 equiv., the different species present in solution seemed to be in or next to the coalescence regime (Figure 3c). A well-defined spectrum characteristic of a single species was ob-

 

tained only after the addition of 9 equiv. of acid (Figure 3f). The latter remained unchanged in the presence of a large excess of acid (ca. 90 equiv. with $Et_3N$), which contrasts with the case of acetic acid. A single set of resonance for the added heptanoic acid was observed, and no high-field-shifted resonance could be detected. The α-methylene protons of heptanoic acid, detectable only after the addition of 2 equiv., showed a low-field shift (CIS = +0.2 ppm; see Table 1). All these observations attest to its coordination to the metal center and a fast exchange regime with free acid. The $Zn^{II}$ ion embedded in the $Rim_3$ ligand displays a much lower affinity for a long-chain acid than for acetic acid and, owing to steric host–guest misfit, it can bind only 1 equiv., instead of 2 equiv. with acetic acid (Scheme 1).

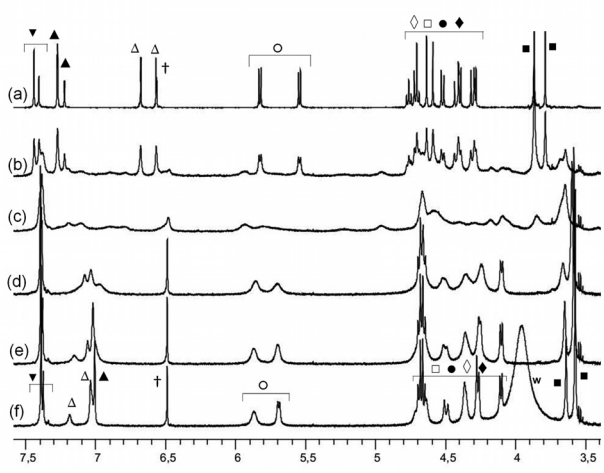


Figure 3. $^1H$ NMR spectra of $[Zn(Rim)(S)_2][ClO_4]_2$ in $CD_3CN$ (500 MHz, 300 K, $c$ = 1.7 mM) before (a) and after the addition of a 1:1.5 mixture of heptanoic acid/triethylamine: (b) 0.4, (c) 0.9, (d) 1.8, (e) 2.8, and (f) 9 equiv. of acid. ▼ HAr "down", ▲ and Δ HIm, † HAr "up", ○ and ● $OCH_2O$, □ $CHC_5H_{11}$, ◇ $CH_2Im$, ♦ $Ar\text{-}CH_2O$, ■ $NCH_3$; w stands for water.

Table 1. Complexation-induced shift values.

| Substrate | $\delta_{free}$[a] | $\delta_{coord}$ | $\Delta\delta$ = CIS |
|---|---|---|---|
| HCOOH | 8.43 | 4.17 | –4.26 |
| $CH_3COOH$ | 1.87 | –2.43 | –4.23 |
| $CH_3CH_2COOH$ *endo* bound | 1.00 | –2.67 | –3.68 |
| $CH_3CH_2COOH$ *exo* bound | 2.11 | ca. 2.3 | ca. +0.2 |
| $CH_3CONH_2$ | 1.84 | –2.26 | –4.12 |
| $nC_5H_{11}CH_2COOH$ | 2.11 | 2.29 | ca. +0.2 |
| $CH_3COCHCOCH_3$ | 2.01[b] | 1.85/–2.45[b] | –0.16/–4.46[b] |
| $CH_3COCHCOCH_3$ | 5.61 | n.d. | –0.35 |
| $CH_3COCHCOPh$ | 2.18 | –2.25 | –4.43 |
| $CH_3COCHCOPh$ | 6.37 | 4.95 | –1.42 |
| $CH_3COCHCOPh$ | (*ortho*) 7.92 | 7.73 | –0.19 |
| | (*para*) 7.53 | 7.63 | + 0.10 |
| | (*meta*) 7.50 | 7.58 | + 0.08 |
| $CH_3COCHCOCH_2CH_3$ | 2.01 | –2.19 | –4.2 |
| $CH_3COCHCOCH_2CH_3$ | 5.62 | n.d. | –0.36 |
| $CH_3COCHCOCH_2CH_3$ | 2.32 | 2.07 | –0.25 |

[a] The $\delta_{free}$ values correspond to $^1H$ NMR resonances in solutions containing both the acidic ligand and triethylamine in a (1:1) ratio. In view of their $pK_a$ values in MeCN (e.g., 18.8 for triethylammonium vs. 23.5 for acetic acid),[23] the ligands are only somewhat deprotonated when they are free, and their $\delta$ values essentially represent their neutral form, whereas when they are bound to the $Zn^{II}$ center, they are anionic. [b] $\delta$ obtained at $T$ = 265 K. n.d.: not determined.

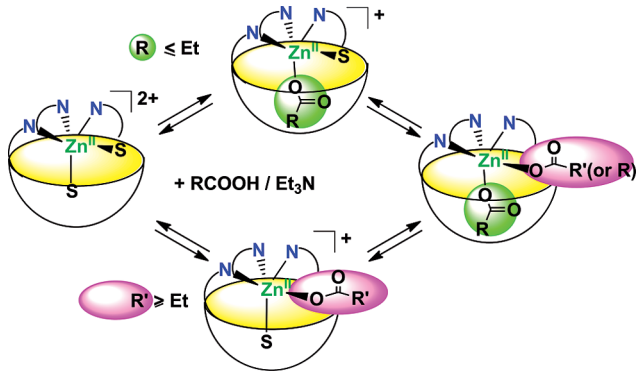


Scheme 1. Selective *endo* vs. *exo* binding of carboxylates to the $Rim_3Zn^{II}$ complex in $CD_3CN$.

## Other Organic Acids – *endolexo* Selectivity

The scope of carboxylate binding to the $Zn^{II}$ bowl complex was further explored. The reaction with formic acid under the same experimental conditions as those described above (in the presence of $Et_3N$) led to the spectrum displayed in Figure 4b. The spectrum shows the clean and quantitative formation of a single species. Careful analysis of the spectrum showed a signal at $\delta$ = 4.17 ppm that integrates for one proton, which was identified as the proton of the encapsulated formate ion (CIS = –4.26 pm) through a saturation transfer experiment. Hence, the shielding effect of the aromatic units towards the encapsulated guest is approximately the same for the proton of the formate ion and the methyl group of the acetate ion. Interestingly, the *endo* coordination of acetate and formate ions was also indirectly evidenced by mass spectrometry (ESI). Mass peaks corresponding to the monocationic species $[Rim_3Zn(OAc)]^+$ and $[Rim_3Zn(OOCH)]^+$ were observed in the case of an *endo* coordination mode, whereas no peaks corresponding to complexes obtained with larger carboxylates (*exo*-coordinated) could be detected under the same experimental conditions. This observation substantiates a stronger complexation of small carboxylates in relation to their *endo* position.

In all cases, the reaction of an aromatic acid such as hippuric acid (bearing a bulky phenyl group) or amino acids such as glycine and alanine resulted in the formation of new species as attested by the corresponding NMR signatures displayed in Figure 4d and e. In each case, the spectrum is similar to that obtained with heptanoic acid and indicates *exo* coordination of the carboxylate donor. Hence, even the relatively small glycine appears too large for the cavity. When propionic acid was tested, a similar signature was obtained when excess acid was added to the solution (Figure 4c). Interestingly, however, under substoichiometric conditions, a small peak was detected at $\delta$ = –2.68 ppm (CIS = –3.68 ppm), which indicates that a small portion of

 

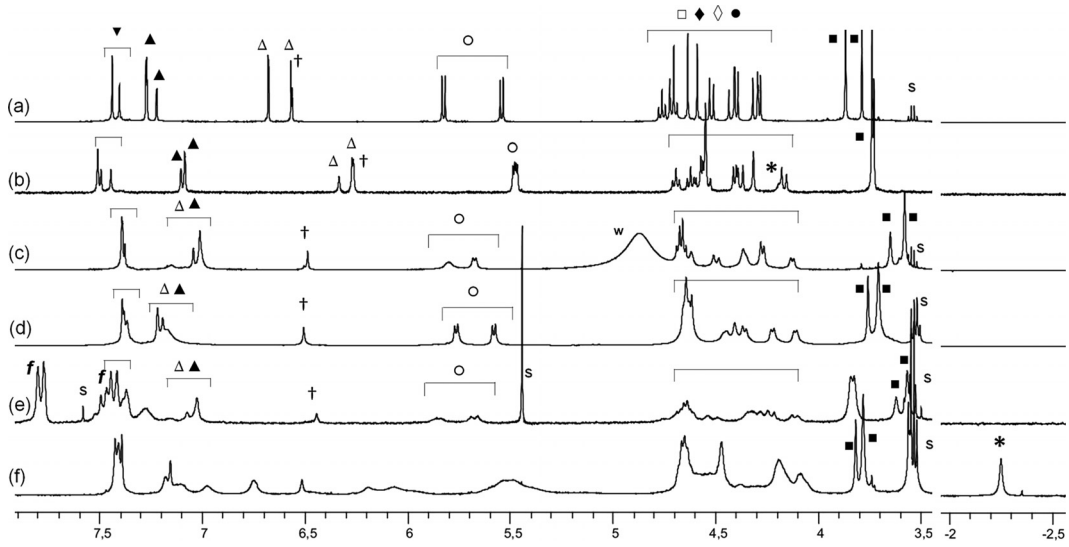


Figure 4. $^1$H NMR spectra of $[Zn(Rim)(S)_2][ClO4]_2$ in $CD_3CN$ (300 K) before (a) and after the addition of (b) 1.5 equiv. of HCOOH/$Et_3N$ (1:1), (c) 9 equiv. of $EtCO_2H/Et_3N$ (1:1.5), (d) 4.5 equiv. of glycine in 15 μL $D_2O$, (e) 5 equiv. of a $CDCl_3$ solution (20 μL) of hippuric acid/$Et_3N$ (1:2), and (f) 2 equiv. of $CH_3CONH_2/Et_3N$ (1:1). The signal annotated with an asterisk corresponds to the encapsulated guest, signals annotated "*f*" stand for the free guest; S stands for solvent, and w stands for water. ▼ HAr "down", ▲ and Δ HIm, † HAr "up", ○ and ● $OCH_2O$, □ $CHC_5H_{11}$, ◇ $CH_2Im$, ♦ $ArCH_2O$, ■ $NCH_3$. All spectra were recorded at 500 MHz, except (e), which was recorded at 250 MHz.

the propionate ions (ca. 10%) were coordinated in the *endo* position. Reasoning that *endo* complexation of a ligand is in competition with *endo* binding of the solvent, we repeated the experiment in an a priori less competitive solvent, acetone, and found indeed that the percentage of *endo* complexation increased to ca. 50% (Figures S4 and S5). This indicates that the propionate ion is a borderline case from a size-fit point of view and leads to an equilibrium between the *endo* and *exo* sites that can be displaced by changing the solvent.

Hence, this overview of carboxylate coordination has highlighted several points:

(1) Depending on its size, the carboxylate ion coordinates either at the *endo* or at the *exo* position. The good fit for *endo* binding corresponds to the acetate ion, although a smaller guest (formate) also prefers the *endo* position. The propionate ion appears to be the limiting size for encapsulation, and larger guests all undergo *exo* coordination. This highlights a very sharp selectivity for *endo* binding (Scheme 1).

(2) The *exo* position allows coordination of carboxylate ions bearing functional groups (amino acids) or bulky substituents (phenyl).

(3) Whereas simultaneous coordination at the *endo* and *exo* positions can be obtained with the acetate ion, coordination appears to be restricted to a 1:1 stoichiometry for larger exogenous ligands.

(4) Coordination at the *endo* position is stronger than at the *exo* position. This shows that embedment strengthens the link between the metal center and the exogenous donor. It also suggests that the p$K_a$ decrease of the carboxylic acid promoted by its interaction with the metal center is more important at the *endo* position than at the *exo* position.

To further test the ability of the $Zn^{II}$ center to lower the p$K_a$ of the exogenous ligand, we tested the coordination of acetamide. Upon the addition of 1 equiv. of acetamide to a solution of the $Rim_3Zn^{II}$ complex in $CD_3CN$, no modification of the $^1$H NMR spectrum occurred. After the addition of triethylamine, the $^1$H NMR spectrum displayed extremely broad resonances over a large temperature range (240–340 K; Figure S7). Interestingly, in addition to these broad NMR signals in the downfield region, a sharp peak in the high-field region was detected ($\delta$ = –2.26 ppm; Figure 4f). This observation indicates the encapsulation of acetamide inside the cavity (CIS = –4.12 ppm).

In spite of the ill-defined spectrum in the $\delta$ = 4–7 ppm region, careful quantification indicated the stoichiometric binding of the amido guest inside the cavity. Hence, the broad resonances obtained for the $Rim_3$ ligand might be attributed to different coordination modes of the deprotonated acetamide to the metal ion (mono- or bidentate, O- or N-coordinated).

### Bidentate Ligands – β-Diketone Coordination

To further characterize the free coordination sites at the $Zn^{II}$ center embedded in the $Rim_3$ ligand, presumed to be in *cis* positions relative to each other, the coordination of bidentate ligands was explored. The reactions of various β-diketones with an acetyl group (for cavity fitting) in the presence of triethylamine with $Rim_3Zn^{II}$ in deuterated acetonitrile were monitored by $^1$H NMR spectroscopy. The addition of a (1:1) mixture of diketone and triethylamine led to a new well-defined NMR profile, which presents sharp peaks characteristic of a complex bisected by a mirror

 

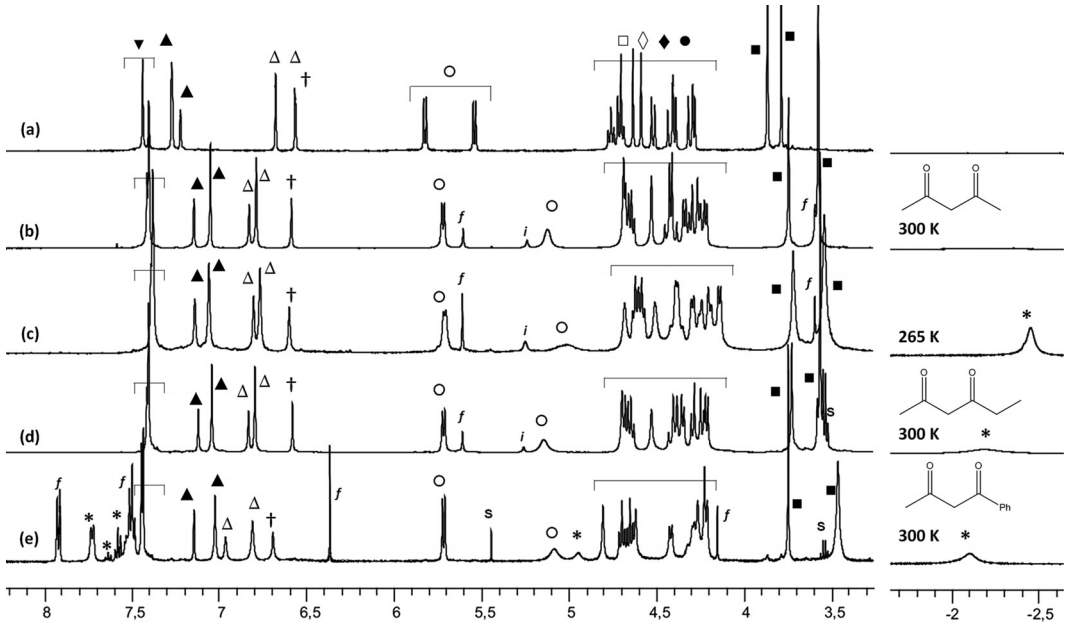


Figure 5. $^1$H NMR spectra (500 MHz) of $[Zn(Rim)(S)_2][ClO_4]_2$ in $CD_3CN$ before (a, 300 K) and after the addition of diketones (2 equiv.) and triethylamine: acetylacetone and 2 equiv. $Et_3N$ relative to Zn at (b) 300 and (c) 265 K, (d) 2,4-hexanedione and 2 equiv. $Et_3N$ at 300 K, and (e) 1-benzoylacetone and 1 equiv. $Et_3N$ at 300 K. ▼ HAr "down", ▲ and Δ HIm, † HAr "up", ○ and ● $OCH_2O$, □ $CHC_5H_{11}$, ◇ $CH_2Im$, ♦ $ArCH_2O$, ■ $NCH_3$. The asterisks correspond to encapsulated guests. Signals annotated with "*f*" correspond to the protons of free diketones. The corresponding $\delta$ values are reported in Table 1; *i* stands for a small impurity, and S indicates residual solvent.

plane. The NMR profiles are rather similar (Figure 5) for the three diketones tested. The signals of the imidazole protons are shifted, and the methylene protons of the lateral imidazole arms are diastereotopic; thus, they are indeed coordinated to the metal center. The two signals corresponding to the *N*-methyl protons of the imidazole groups are shifted upfield, which denotes a change of their environment. The NMR signals corresponding to the methylene bridges of the large rim of the bowl are also strongly affected, and this can be correlated to the presence of the half-embedded bidentate guest. All these observations are consistent with the formation of a complex with a symmetry plane with two equivalent imidazole arms at both sides of the mirror plane and one imidazole group and the enolate guest orientated in the symmetry plane. Finally, the coordination of these diketones was further evidenced by ESI-MS spectrometry; in each case, a peak corresponding to the monocationic host–guest adduct $[Rim_3Zn(CH_3COCHCOR)]^+$ (R = Me, Et, and Ph) was observed.

For each diketone, an upfield-shifted resonance corresponding to the embedded acetyl group was observed at $\delta < -2$ ppm. Saturation transfer experiments showed that they are in exchange with free diketones, a process that is clearly slow for propionyl and benzoyl acetate at 300 K on the spectroscopic timescale (Figure 5d and e). In these two cases, the broadness of the *endo*-bound methyl peak at 300 K does not seem to be associated with the intermolecular exchange process in view of the sharpness of the other resonances associated with the guest, such as those of the phenyl group in the low-field region (Figure 5e). Lowering the temperature led to a sharpening of the high-field methyl peaks but also to a broadening of the imidazole resonances (Figure S13). This is suggestive of conformational exchange between stereoisomers at the level of the first coordination sphere of the $Zn^{II}$ center. Surprisingly, however, in the case of acetylacetonate, the peak at $\delta = -2$ ppm is observable only at low *T* (Figure 5b and c). A detailed variable-temperature study (Figure 6) shows that two signals gradually and simultaneously appear as the temperature decreases.

At 240 K, the resonances at $\delta = 1.85$ and $-2.55$ ppm are sharp, and each integrates for three protons. These two peaks are confidently attributed to the two methyl groups of the guest, which experience a different shielding effect by the resorcinarene core owing to their different spatial position (*exo* and *endo*, respectively). Saturation transfer experiments showed that these two methyl groups are in exchange with each other (irradiation at $\delta = -2.55$ ppm leads to the disappearance of the resonance at $\delta = 1.85$ ppm and vice versa) and that the methyl groups of free acetylacetone are in exchange with those of the bound guest (irradiation at $\delta = 2.01$ ppm leads to the disappearance of both high-field peaks at $\delta = -2.55$ ppm and 1.85 ppm). Interestingly, over the whole temperature range, the sharpness of the peaks corresponding to free acetylacetone does not appear to be affected (Figure 6). This suggests the existence of a different exchange mechanism (Scheme 2): in addition to the intermolecular exchange, the guest undergoes an intramolecular exchange, and its *endo* and *exo* methyl groups switch positions. According to the NMR spectroscopic data, this intramolecular process is faster than the intermolecular exchange. For propionyl- and benzoylacetone, the intramolec-

 

ular *endo–exo* exchange is not observed because of the presence of one sterically hindered group on one side of the diketone, the embedment of which is either disfavored compared to acetyl or precluded for steric reasons. Thus, these two diketones only undergo intermolecular exchange (Scheme 2). As a consequence, the signal of their inward-orientated methyl groups is observable at higher temperature (300 K; Figure 5d and e).

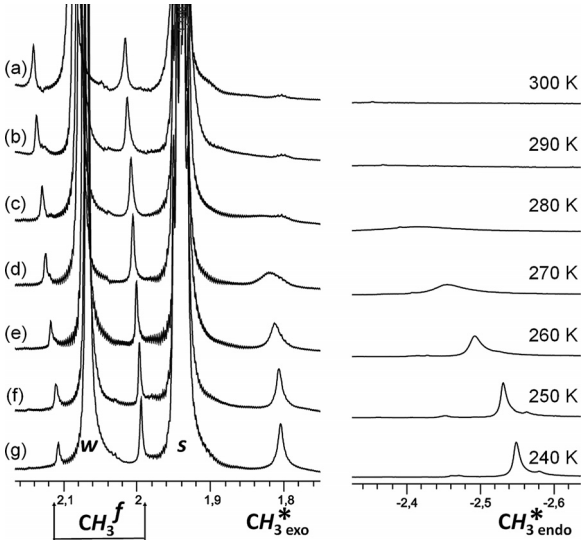


Figure 6. $^1$H NMR spectra (500 MHz) of $[Zn(Rim)(S)_2][ClO_4]_2$ in $CD_3CN$ in the presence of 2 equiv. of acetylacetone/$Et_3N$ (1:1) at various temperatures. Peaks annotated with * are those of the protons of the coordinated acetylacetonate guest. Signals annotated by "*f*" correspond to the protons of free diketone present as a mixture of tautomeric forms (keto-enol and diketone).

Hence, the study of the coordination of diketones has shown the following:

(1) They readily bind to the metal center to form five-coordinate species, which are bound to the three imidazole groups and the deprotonated diketone.

(2) Coordination of these bidentate ligands unambiguously demonstrates the presence of two labile sites on the dicationic complex in *cis* positions relative to each other.

(3) Once bound, the two methyl groups of acetylacetonate are differentiated owing to the embedment of one of them inside the bowl cavity.

(4) Nonsymmetrical diketones bearing an acetyl moiety are selectively bound in the orientation that positions the methyl groups inside the cavity.

(5) Bulky groups such as a benzoyl moiety can occupy only the *exo* position.

(6) In addition to intermolecular exchange of diketone ligands, a very unusual intramolecular exchange process was identified: the two methyl groups of the acetylacetonate guest exchange between the *endo* and *exo* positions.

The structures of the $Zn^{II}$ bowl complexes are further highlighted by the comparison of the CIS values measured for the various ligands. These data are listed in Table 1. When a methyl group is present in the β position relative to the donor atom, it is embedded in the cavity. The similarity of the corresponding CIS values (ca. –4 ppm) indicates that they are similarly positioned in the cavity, in spite of the variety of patterns present in the *exo* position (solvent

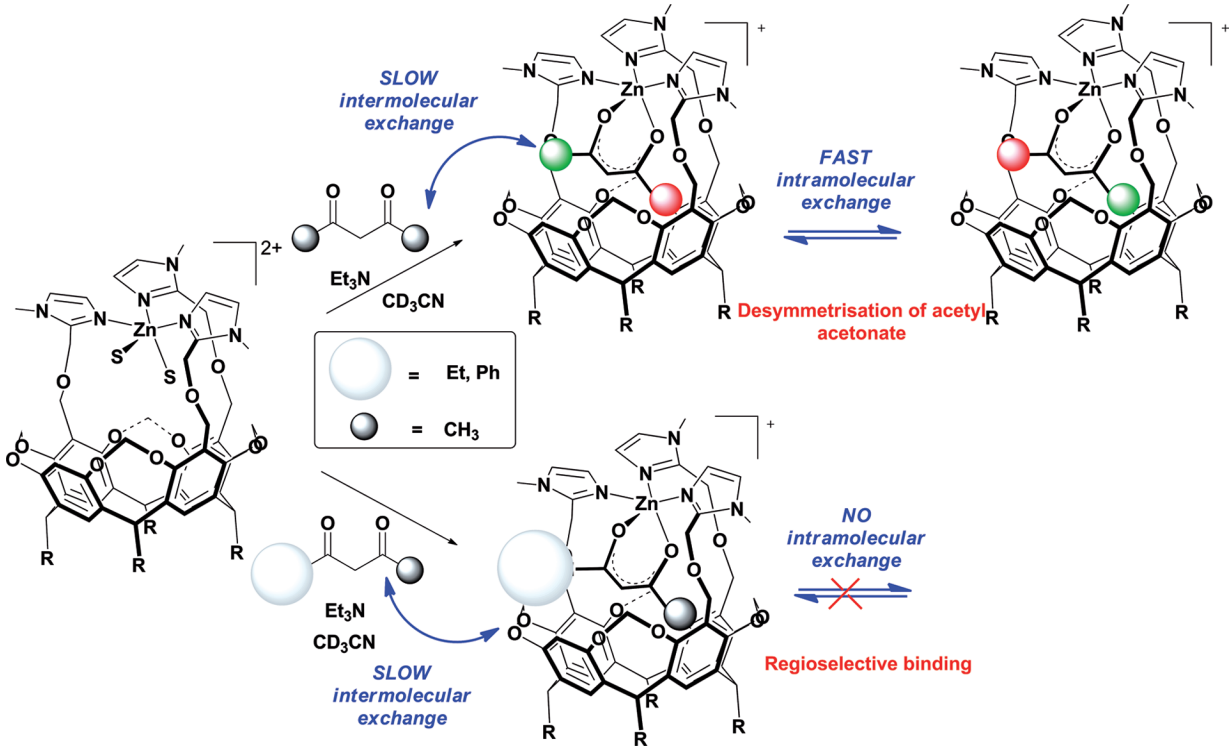


Scheme 2. Schematic representation of the intra- and intermolecular exchange in the case of symmetrical and unsymmetrical 1,3-diketonates bound to the $Rim_3Zn^{II}$ complex.

 

for carboxylates, benzoyl, and propionyl or acetyl donors for diketonates). This emphasizes the relatively strong interaction of the embedded methyl group with the four aromatic units of the cavity that dictates the positioning of the guest. As the imidazole arms are flexible, they adapt to the other part of the guest. This is further reflected by the CIS value for formate, which is similar to that of acetate. This suggests that this guest is more deeply included in the bowl, again to optimize stabilizing CH–π interactions. Such behavior is different from that reported for the funnel $Zn^{II}$ receptors based on calix[6]arene: in that case, the position of the guest in the cone cavity correlated to its position relative to the donor atom bound to the metal center at the level of the small rim of the cone (Figure 1).[7] This was evidenced by the CIS values of the guest, which actually indicated where the protons were situated relative to the metal center. With the more rigid bowl, which is closed at the small rim of the macrocycle, CH–π interactions at its bottom seem to dictate the position of the guest (third coordination sphere), and as a consequence, that of the bound donor atom, which in turn must define the position of the metal ion. Indeed, the great variability of the imidazole pattern in the NMR spectra of the host–guest adducts (Figures 2, 3, and 4) conveys the variation of their environment.

## Conclusions

This study has shown that the resorcinarene-based tris(imidazole) ligand $Rim_3$ allows the stabilization of a dicationic $Zn^{II}$ complex in a five-coordinate environment that is prone to the exogenous binding of two donors. The coordination of various carboxylate ions has evidenced two different interaction sites. The *endo* position displays a distinct size selectivity that allows the strong binding of formate and acetate ions, whereas the major site of interaction for propionate ions is the *exo* position. In contrast, the *exo* position allows the binding of large carboxylate ions. As a result, although the complex can bind two small carboxylate ions (e.g., acetate), it binds a single large carboxylate ion (e.g., hippurate). Titration experiments also evidenced a much stronger binding of small carboxylate ions at the *endo* position than at *exo* the position. The relative *cis* position of the two labile sites present on the $Rim_3Zn^{II}$ complex has been clearly evidenced by the regioselective coordination of nonsymmetrical β-diketones with an acetyl group, which is selectively bound in the *endo* position. Interestingly, the coordination of acetylacetone leads to its desymmetrization, and the two differentiated methyl groups undergo intramolecular exchange.

A comparison with $Zn^{II}$ funnel complexes highlights the drastic differences in the properties of the metal ion when it is embedded in a cone or in a bowl ($Xim_3$ and $Rim_3$, respectively; Figure 1c and d):

(1) The $Zn^{II}$ ion coordinated to the tris(imidazole) core provided by the calix[6]arene-based ligand $Xim_3$ is constrained in a four-coordinate $T_d$ environment, which confers a strong Lewis acidity to the $Zn^{II}$ ion. As a result, the $Xim_3Zn^{II}$ complexes display remarkable affinities for a variety of neutral donors as weak as acetaldehyde.[7,8] However, the funnel provides a very different second coordination sphere compared to that of the bowl: its oxygen-rich small rim acts as a repellent for anions at the *endo* position.[11] This leads to drastically different behaviors: acetic acid and acetamide coordinate within funnels,[7] stabilized by H bonding at the small rim, whereas acetate and deprotonated acetamide anions coordinate within the bowl.

(2) Both systems display very different size selectivities: the bowl accepts a donor three atoms long (acetyl) or smaller, whereas the funnel, which is open at its large rim, can host very large guests provided that part of it fits in the narrow rim of the cone.[8]

(3) Whereas the small rim of the calixarene precludes bidentate coordination modes, the bowl readily allows it.

(4) With some other metal ions ($Cu^{II}$, $Ni^{II}$, and $Co^{II}$), calixarene-based complexes present a second coordination site that is accessible to small exogenous donors[21] like the bowls (although the bowl accepts large donors in the *exo* position). However, this second site of interaction is in a *trans* position relative to the *endo* site, whereas the bowl favors *cis* coordination.

(5) With funnel complexes, the metal ion dictates the position of the guest in the cavity.[7] With bowl complexes, the cavity dictates the position of the metal center through its interaction with the guest.

In conclusion, this study has highlighted the importance that a cavity can have for controlling the properties of metal ions and, hence, reactivity. Within the same biomimetic first coordination sphere provided by three imidazole donors grafted at the rim of a cavity, the $Zn^{II}$ ion has been shown to display drastically different properties in the bowl and in the funnel systems. Both the shape of the cavity (third coordination sphere) and the second coordination sphere that it provides have been shown to play major roles in defining the properties of the metal center. To the best of our knowledge, the bowl system is the first supramolecular system (a cavity complex) to display two well-identified and differentiated labile sites that are prone to the selective binding of two different exogenous donors in *cis* positions relative to each other. Such a feature makes the reactivity of the system full of promise, and this is currently under exploration in our group.

## Experimental Section

**Materials:** The one- and two-dimensional $^1H$ and $^{13}C$ NMR spectra were recorded with an Avance 500 spectrometer (500 MHz). The $^1H$ and $^{13}C$ chemical shifts ($\delta$) were referenced to $SiMe_4$. Standard heteronuclear single quantum coherence (HSQC) and HMBC experiments were used for peak assignments. MS (ESI) analyses were obtained with a ThermoFinnigen LCQ Advantage spectrometer with methanol, dichloromethane, or acetonitrile as solvents. IR spectra were obtained with a Perkin–Elmer Spectrum One FTIR spectrometer equipped with a MIRacle™ single-reflection horizontal attenuated total reflectance (ATR) unit (germanium crystal).

**[Zn(Rim)(OOCH)]$^+$:** Complex $[Zn(Rim)(H_2O)(ClO_4)][ClO_4]_2$ was dissolved in $CD_3CN$. To the resulting dicationic complex [Zn(Rim)-

 

$(MeCN)_2][ClO_4]_2$, an equimolar mixture of triethylamine and formic acid was then added ($c$ = 3 mM in an NMR tube). $^1$H NMR (500 MHz, $CD_3CN$, 25 °C): $\delta$ = 0.93 (m, 12 H, $CH_3$), 1.26–1.47 [m, 24 H, $(CH_2)_3$], 2.34 (m, 8 H, $CH_2CH$), 3.73 (s, 3 H, $ImCH_3$), 3.74 (s, 6 H, $ImCH_3$), 4.17 ($HCOO_{in}$), 4.30–4.43 (m, 8 H, $OCH_{2,in}O$, $ArCH_2O$), 4.53–4.59 (m, 8 H, $OCH_{2,in}O$, $ImCH_2O$), 4.62 and 4.69 (t, $^3J_{H,H}$ = 8.0 Hz, 4 H, $CH_2CH$), 5.47 and 5.48 [2 d, $^3J_{H,H}$ = 7.6 Hz, 4 H, $OCH_{2,out}O$], 6.26 (s, 2 H, ImH), 6.27 (s, 1 H, ArH up), 6.34 (s, 1 H, ImH), 7.09 (s, 2 H, ImH), 7.11 (s, 1 H, ImH), 7.45 (s, 1 H, ArH low), 7.49 (s, 1 H, ArH low), 7.51 (s, 2 H, ArH low) ppm.

**$[Zn(Rim)(CH_3COCHCOCH_3)]^+$:** An equimolar mixture containing triethylamine and acetylacetone (2 equiv.) was added to a solution of $[Zn(Rim)(MeCN)_2][ClO_4]_2$ in $CD_3CN$ ($c$ = 3.0 mM in an NMR tube). $^1$H NMR (500 MHz, $CD_3CN$, 25 °C): $\delta$ = –2.23 (very br. s, 3 H, $CH_{3,in}COCHCOCH_3$), 0.91 and 0.92 (2 t, $^3J_{H,H}$ = 7.1 Hz, 12 H, $CH_3$), 1.26–1.48 [m, 24 H, $(CH_2)_3$], 1.80 (very br. s, 3 H, $CH_{3,in}COCHCOCH_3$), 2.01 [s, free $CH_3COCHC(OH)CH_3$], 2.14 (s, free $CH_3COCH_2COCH_3$), 2.33 (m, 8 H, $CH_2CH$), 3.58 (s, 6 H, $ImCH_3$), 3.60 (s, free $CH_3COCH_2COCH_3$), 3.75 (s, 3 H, $ImCH_3$), 4.15–4.77 (m, 20 H, $ImCH_2O$, $CH_2CH$, $ArCH_2O$, $OCH_{2,in}O$), 5.12 (br. s, 2 H, $OCH_{2,out}O$), 5.61 [s, free $CH_3COCHC(OH)CH_3$], 5.73 (d, $^3J_{H,H}$ = 7.4 Hz, 2 H, $OCH_{2,out}O$), 6.59 (s, 1 H, ArH up), 6.79 (s, 2 H, ImH), 6.83 (s, 1 H, ImH), 7.15 (s, 1 H, ImH), 7.05 (s, 2 H, ImH), 7.40 (s, 3 H, ArH low), 7.42 (s, 1 H, ArH low) ppm. ESI-MS ($CH_3CN$): $m/z$ = 676.3 $[Zn(Rim)(CH_3COCH_2COCH_3)]^{2+}$, 1351.5 $[Zn(Rim)(CH_3COCHCOCH_3)]^+$.

**$[Zn(Rim)(CH_3COCHCOCH_2CH_3)]^+$:** An equimolar mixture containing triethylamine and hexane-2,4-dione (2 equiv.) was added to a solution of $[Zn(Rim)(MeCN)_2][ClO_4]_2$ in $CD_3CN$ ($c$ = 3.0 mM in an NMR tube). $^1$H NMR (500 MHz, $CD_3CN$, 25 °C): $\delta$ = –2.19 (br. s, 3 H, $CH_{3,in}COCHCOEt$), 0.92 and 0.93 (2 t, $^3J_{H,H}$ = 7.1 Hz, 12 H, $CH_3$), 0.97 and 1.08 [s, free $MeCOCHC(OH)CH_2CH_3$], 1.24–1.47 [m, 24 H, $(CH_2)_3$], 2.08 [s, free $EtCOCHC(OH)CH_3$], 2.14 (s, free $EtCOCH_2COCH_3$), 2.36 (m, 8 H, $CH_2CH$), 2.47 [s, free $MeCOCHC(OH)CH_2CH_3$], 3.56 (s, 6 H, $ImCH_3$), 3.58 (s, free $CH_3COCH_2COEt_3$), 3.73 (s, 3 H, $ImCH_3$), 4.14–4.74 (m, 20 H, $ImCH_2O$, $CH_2CH$, m, $ArCH_2O$, $OCH_{2,in}O$), 5.15 (br. s, 2 H, $OCH_{2,out}O$), 5.62 [s, free $CH_3COCHC(OH)Et$], 5.72 (d, $^3J_{H,H}$ = 7.3 Hz, 2 H, $OCH_{2,out}O$), 6.58 (s, 1 H, ArH up), 6.84 (s, 1 H, ImH), 6.81 (s, 2 H, ImH), 7.05 (s, 2 H, ImH), 7.12 (s, 1 H, ImH), 7.41 (s, 3 H, ArH low), 7.42 (s, 1 H, ArH low) ppm.

**$[Zn(Rim)(CH_3COCHCOPh)]^+$:** 1-Benzoylacetone (2 equiv.) in $CD_3CN$ was added to a solution of $[Zn(Rim)(MeCN)_2][ClO_4]_2$ in $CD_3CN$ ($c$ = 4.3 mM) in an NMR tube, followed by the addition of triethylamine (1 equiv.). $^1$H NMR (500 MHz, $CD_3CN$, 25 °C): $\delta$ = –2.10 [br. s, 3 H, bound $CH_3COCHC(O)Ph$], 0.92 and 0.93 (2 t, $^3J_{H,H}$ = 7.1 Hz, 12 H, $CH_3$), 1.48–1.26 [m, 24 H, $(CH_2)_3$], 2.18 [s, free $PhCOCHC(OH)CH_3$], 2.23 (s, free $PhCOCH_2COCH_3$), 2.36 (m, 8 H, $CH_2CH$), 3.46 (s, 6 H,$ImCH_3$), 3.75 (s, 3 H, $ImCH_3$), 4.15 (s, free $CH_3COCH_2COPh$), 4.18–4.84 (m, 20 H, $ImCH_2O$, $CH_2CH$, $ArCH_2O$, $OCH_{2,in}O$), 4.95 [s, 1 H, bound $CH_3COCHC(O)Ph$], 5.09 (m, 2 H, $OCH_{2,out}O$), 5.72 (d, $^3J_{H,H}$ = 7.4 Hz, 2 H, $OCH_{2,out}O$), 6.37 [free $CH_3COCHC(OH)Ph$], 6.70 (s, 1 H, ArH up, s), 6.81 (s, 2 H, ImH), 6.97 (s, 1 H, ImH), 7.03 (s, 2 H, ImH), 7.15 (s, 1 H, ImH), 7.38–7.67 (m, free and bound $CH_{meta}PhArH$, free and bound $CH_{ortho}Ph$, ArH low), 7.72 (d, $^3J_{H,H}$ = 7.7 Hz, 2 H, coord. $CH_{ortho}Ph$), 7.92 (d, $^3J_{H,H}$ = 7.7 Hz, free $CH_{ortho}Ph$) ppm.

**Supporting Information** (see footnote on the first page of this article): NMR and ESI mass spectra.

## Acknowledgments

This project was supported by the Centre National de la Recherche Scientifique (CNRS) (Institut de Chimie), the Ministère de l'Enseignement Supérieur et de la Recherche, and the Agence Nationale pour la Recherche [Cavity-zyme(Cu) Project No. ANR-2010-BLAN-7141].

[1] R. Gramage-Doria, D. Armspach, D. Matt, *Coord. Chem. Rev.* **2013**, *257*, 776–816.
[2] For cavities formed upon metal complexation by non-cavity-shaped macrocyclic ligands, see: a) B. Kersting, *Z. Anorg. Allg. Chem.* **2004**, *630*, 765–780; b) B. Kersting, U. Lehmann, "Chemistry of Metalated Container Molecules" in *Advances in Inorganic Chemistry*, vol. 61 (Eds.: R. van Eldik, C. D. Hubbard), Elsevier, The Netherlands, **2009**, p. 407.
[3] For cavities covalently linked to metals other than transition elements, see: a) J. L. Atwood, L. J. Barbour, M. J. Hardie, C. L. Raston, *Coord. Chem. Rev.* **2001**, *222*, 3–32; b) J. T. Lenthall, J. W. Steed, *Coord. Chem. Rev.* **2007**, *251*, 1747–1760.
[4] For a very recent example, see: M. Guitet, P. Zhang, F. Marcelo, C. Tugny, J. Jiménez-Barbero, O. Buriez, C. Amatore, V. Mouriès-Mansuy, J.-P. Goddard, L. Fensterbank, Y. Zhang, S. Roland, M. Ménand, M. Sollogoub, *Angew. Chem. Int. Ed.* **2013**, *52*, 7213–7218; *Angew. Chem.* **2013**, *125*, 7354.
[5] S. Blanchard, L. Le Clainche, M.-N. Rager, B. Chansou, J. P. Tuchagues, A. Duprat, Y. Le Mest, O. Reinaud, *Angew. Chem. Int. Ed.* **1998**, *37*, 2732–2735; *Angew. Chem.* **1998**, *110*, 2861.
[6] C. Wieser-Jeunesse, D. Matt, A. De Cian, *Angew. Chem. Int. Ed.* **1998**, *37*, 2861–2864; *Angew. Chem.* **1998**, *110*, 3027.
[7] O. Sénèque, M.-N. Rager, M. Giorgi, O. Reinaud, *J. Am. Chem. Soc.* **2000**, *122*, 6183–6189.
[8] D. Coquière, S. Gac, U. Darbost, O. Sénèque, I. Jabin, O. Reinaud, *Org. Biomol. Chem.* **2009**, *7*, 2485–2500.
[9] The term "exogenous" is used here to designate ligands with which the cavity complex interacts, in contrast to the cavity ligand itself, which can be considered as "endogenous" to the complex.
[10] a) L. Le Clainche, M. Giorgi, O. Reinaud, *Inorg. Chem.* **2000**, *39*, 3436–3437; b) L. Le Clainche, Y. Rondelez, O. Sénèque, S. Blanchard, M. Campion, M. Giorgi, A. F. Duprat, Y. Le Mest, O. Reinaud, *C. R. Acad. Sci., Ser. IIc: Chim.* **2000**, *3*, 811–819.
[11] G. Izzet, Y. M. Frapart, T. Prangé, K. Provost, A. Michalowicz, O. Reinaud, *Inorg. Chem.* **2005**, *44*, 9743–9751.
[12] a) A. Zanotti-Gerosa, E. Solari, L. Giannini, C. Floriani, N. Re, A. Chiesi-Villa, C. Rizzoli, *Inorg. Chim. Acta* **1998**, *270*, 298–311; b) F. Corazza, C. Floriani, A. Chiesi-Villa, C. Guastini, *J. Chem. Soc., Chem. Commun.* **1990**, 640–641; c) F. Corazza, C. Floriani, A. Chiesi-Villa, C. Rizzoli, *Inorg. Chem.* **1991**, *30*, 4465–4468; d) A. Arduini, C. Massera, A. Pochini, A. Secchi, F. Ugozzoli, *New J. Chem.* **2006**, *30*, 952–958; e) P. Mongrain, J. Douville, J. Gagnon, M. Drouin, A. Decken, D. Fortin, P. D. Harvey, *Can. J. Chem.* **2004**, *82*, 1452–1461; f) V. C. Gibson, C. Redshaw, W. Clegg, M. R. J. Elsegood, *J. Chem. Soc., Chem. Commun.* **1995**, 2371–2372.
[13] a) E. Engeldinger, D. Armspach, D. Matt, *Angew. Chem. Int. Ed.* **2001**, *40*, 2526–2529; b) E. Engeldinger, D. Armspach, D. Matt, P. G. Jones, *Chem. Eur. J.* **2003**, *9*, 3091–3105.
[14] D. Armspach, D. Matt, F. Peruc, P. Lutz, *Eur. J. Inorg. Chem.* **2003**, 805–809.
[15] a) I. Bertini, H. B. Gray, E. I. Stiefel, J. S. Valentine in *Biological Inorganic Chemistry, Structure and Reactivity*, University Science Books, Sausalito, **2007**; b) S. J. Lippard, J. M. Berg in *Principles of Bioinorganic Chemistry*, University Science Books, Mill Valley, **1994**; c) R. H. Holm, P. Kennepohl, E. I. Solomon, *Chem. Rev.* **1996**, *96*, 2239–2314.
[16] a) W. N. Lipscomb, N. Sträter, *Chem. Rev.* **1996**, *96*, 2375–2433; b) G. Parkin, *Chem. Rev.* **2004**, *104*, 699–767.

 

[17] a) M. M. Abu-Omar, A. Loaiza, N. Hontzeas, *Chem. Rev.* **2005**, *105*, 2227–2252; b) L. Que, *Acc. Chem. Res.* **2007**, *40*, 493–500.
[18] a) J.-N. Rebilly, O. Reinaud, *Supramol. Chem.* **2014**, DOI: 10.1080/10610278.2013.877137; b) J.-N. Rebilly, O. Reinaud in *Supramolecular Chemistry: From Molecules to Nanomaterials*, vol. 4 (Eds.: P. A. Gale, J. W. Steed), Wiley, **2012**, p. 1771.
[19] For some recent developments with host–guest systems based on tris(imidazolyl)calix[6]arene complexes, see: a) D. Coquière, A. de la Lande, O. Parisel, T. Prangé, O. Reinaud, *Chem. Eur. J.* **2009**, *15*, 11912–11917; b) D. Coquière, A. de la Lande, S. Martí, O. Parisel, T. Prangé, O. Reinaud, *Proc. Natl. Acad. Sci. USA* **2009**, *106*, 10449–10454; c) C. Monnereau, J.-N. Rebilly, O. Reinaud, *Eur. J. Org. Chem.* **2011**, 166–175.
[20] For host–guest complexes based on calix[6]azacryptands, see: a) U. Darbost, M.-N. Rager, S. Petit, I. Jabin, O. Reinaud, *J. Am. Chem. Soc.* **2005**, *127*, 8517–8525; b) X. Zeng, D. Coquière, A. Alenda, E. Garrier, T. Prangé, Y. Li, O. Reinaud, I. Jabin, *Chem. Eur. J.* **2006**, *12*, 6393–6402; c) D. Over, A. de la Lande, X. Zeng, O. Parisel, O. Reinaud, *Inorg. Chem.* **2009**, *48*, 4317–4330.
[21] O. Sénèque, M. Campion, M. Giorgi, Y. Le Mest, O. Reinaud, *Eur. J. Inorg. Chem.* **2004**, 1817–1826.
[22] A. Višnjevac, J. Gout, N. Ingert, O. Bistri, O. Reinaud, *Org. Lett.* **2010**, *12*, 2044–2047.
[23] a) I. Kaljurand, A. Kütt, L. Sooväli, T. Rodima, V. Mäemets, I. Leito, I. A. Koppel, *J. Org. Chem.* **2005**, *70*, 1019–1028; b) F. Eckert, I. Leito, I. Kaljurand, A. Kütt, A. Klamt, M. Diedenhofen, *J. Comput. Chem.* **2009**, *30*, 799–810.

Received: February 24, 2014
Published Online: May 14, 2014

 